Cosmology and Nuclear Physics

A. Coc

PROCEEDINGS OF SCIENCE

Cosmology and Nuclear Physics

Alain Coc*
Centre de Spectrométrie Nucléaire et de Spectrométrie de Masse (CSNSM), CNRS/IN2P3, Université Paris Sud 11, UMR 8609, Bâtiment 104, F–91405 Orsay Campus, France
E-mail: Alain.Coc@csnsm.in2p3.fr

There are important aspects of Cosmology, the scientific study of the large scale properties of the universe as a whole, for which nuclear physics can provide insights. Here, we will focus on the properties of early universe (Big-Bang nucleosynthesis during the first 20 mn) and on the *variation of constants* over the age of the universe.

VI European Summer School on Experimental Nuclear Astrophysics, ENAS 6
September 18-27, 2011
Acireale Italy

*Speaker.

PoS(ENAS 6)017

1. Introduction

Primordial nucleosynthesis is one of the three observational evidences for the Big–Bang model. Even though they span a range of nine orders of magnitude, there is indeed a good overall agreement between primordial abundances of ^{4}He, D, ^{3}He and ^{7}Li either deduced from observations or from primordial nucleosynthesis calculations. This comparison was used for the determination of the baryonic density of the Universe. For this purpose, it is now superseded by the analysis of the CMB anisotropies. Big–Bang nucleosynthesis remains, nevertheless, a valuable tool to probe the physics of the early Universe. (See also T. Kajino's lecture, earlier contributions to this school [1] or other school [2], and textbooks on cosmology e.g. [3, 4].)

The equivalence principle is a cornerstone of metric theories of gravitation and in particular of General Relativity. This principle, including the universality of free fall and the local position and Lorentz invariances, postulates that the local laws of physics, and in particular the values of the dimensionless constants such as the fine structure constant (α_{em}), must remain fixed, and thus be the same at any time and in any place. It follows that by testing the constancy of fundamental constants one actually performs a test of General Relativity, that can be extended on astrophysical and cosmological scales. (See recent reviews [5, 6].)

2. Primordial nucleosynthesis

There are presently three observational evidences for the Big–Bang Model: the universal expansion, the Cosmic Microwave Background radiation (CMB) and Primordial or Big-Bang Nucleosynthesis (BBN). Prominent landmarks in the development of the Big Bang nucleosynthesis theory include works by Gamow in the 1940's (out of equilibrium nucleosynthesis in an expanding Universe dominated by radiation), Peebles in 1966 (Big Bang nucleosynthesis calculations up to ^{4}He) and Wagoner in 1973 (Big Bang nucleosynthesis calculations including ^{7}Li).

It is worth reminding that even though it has now been superseded, for these purposes, BBN used to be the only constraints on the baryonic density of the universe and on the number of neutrino families. Now that these quantities have been more precisely determined by the WMAP and LEP experiments, BBN remains a powerful tool to probe the early Universe or to test fundamental physics.

2.1 The Big–Bang model

Galaxies are observed to be receding from us with a velocity V_{rec}, proportional to distance D. This is summarized by the Hubble law: $V_{rec} = H_0 \times D$ where H_0 is called the Hubble parameter. The Hubble law can be considered as a direct consequence of the expansion of the universe assuming that spatial dimensions are all proportional to a scale factor $a(t)$ that increases with time. An other consequence of the expansion is that the wavelengths also scale as a so that a radiation emitted with a wavelength λ is now observed with a wavelength λ_0. It defines the *redshift* z of the source:

$$z \equiv \lambda_0/\lambda - 1 = a_0/a - 1 \tag{2.1}$$

where a and a_0 are the scale factors respectively at emission and present times[1]. A modern determination of the Hubble constant leads to $H_0 \approx 70$ km/s/Mpc [2]. It is usual to parameterize H_0 as $H_0 = h \times 100$ km/s/Mpc with $h \approx 0.70$.

Recombination of the free electrons with protons occurs when the temperature drops below 3000 K. Space, now filled with neutral atoms, becomes transparent for the first time and thermalized photons are free to roam the Universe. Because of the expansion, photons are affected by redshift so that their present temperature has now dropped to 2.725 K. This radiation is hence now in the microwave domain and is called Cosmic Microwave Background radiation (CMB). The evolution with temperature of the fraction of ionized hydrogen atoms $X_e \equiv n_e^- / (n_p + n_H)$ is given by the Saha equation [4]:

$$\frac{X_e^2}{1 - X_e^2} = \left(\frac{m_e c^2 \mathrm{k}_B T}{2\pi(\hbar c)^2} \right)^{\frac{3}{2}} \frac{\exp -\frac{E_I}{\mathrm{k}_B T}}{n_B} \tag{2.2}$$

with the approximation of a pure ^{1}H gas. At this epoch (radiation dominated), the baryon number and temperature evolve as $n_B = n_p + n_H \propto a^{-3}(t)$ and $T \propto a^{-1}(t)$ (see next section). Figure 1 shows that, with these approximations, the fraction of ionized hydrogen drops abruptly around T = 3000–4000 K, much lower than the ionisation energy: E_I = 13.6 eV (1.6×10^5 K).

The third evidence for a hot Big–Bang comes from the primordial abundances of the "light elements": ^{4}He, D, ^{3}He and ^{7}Li. They are produced in the first ≈20 mn of the Universe when it was dense and hot enough for nuclear reactions to take place. Starting from protons and neutrons, it leads mainly to ^{4}He and stops at mass A=7 because A=5 and 8 nuclei, being particle unbound, have too short lifetimes. These primordial abundances can, in principle, be deduced from astronomical observations of objects that were formed shortly after the Big–Bang. When compared with Big–Bang Nucleosynthesis (BBN) calculations, the overall agreement spans nine orders of magnitudes! The number of free parameters entering Standard Big–Bang Nucleosynthesis have decreased with

Table 1: Density components of the Universe

Radiation (CMB) energy	$\Omega_{R(CMB)}$	5×10^{-5}
Visible matter	Ω_L	≈ 0.003
Baryonic matter	Ω_B	0.046
Matter (dark+baryonic)	Ω_M	0.27
Vacuum energy	Ω_Λ	0.73
Total	Ω_T	1.00

time. The number of light neutrino families is known from the measurement of the Z^0 width by LEP experiments at CERN [7]. The lifetime of the neutron (entering in weak reaction rate calculation) and the nuclear reaction rates have been measured in nuclear physics laboratories [8]. The last parameter to have been independently determined is the baryonic density of the Universe which is now deduced from the observations of the anisotropies of the CMB radiation [9]. When considering density components of the Universe, it is convenient to refer to the *critical density*

[1] Present values are usually labeled with index 0

[2] Mpc (megaparsec) = 3.26×10^6 light-years

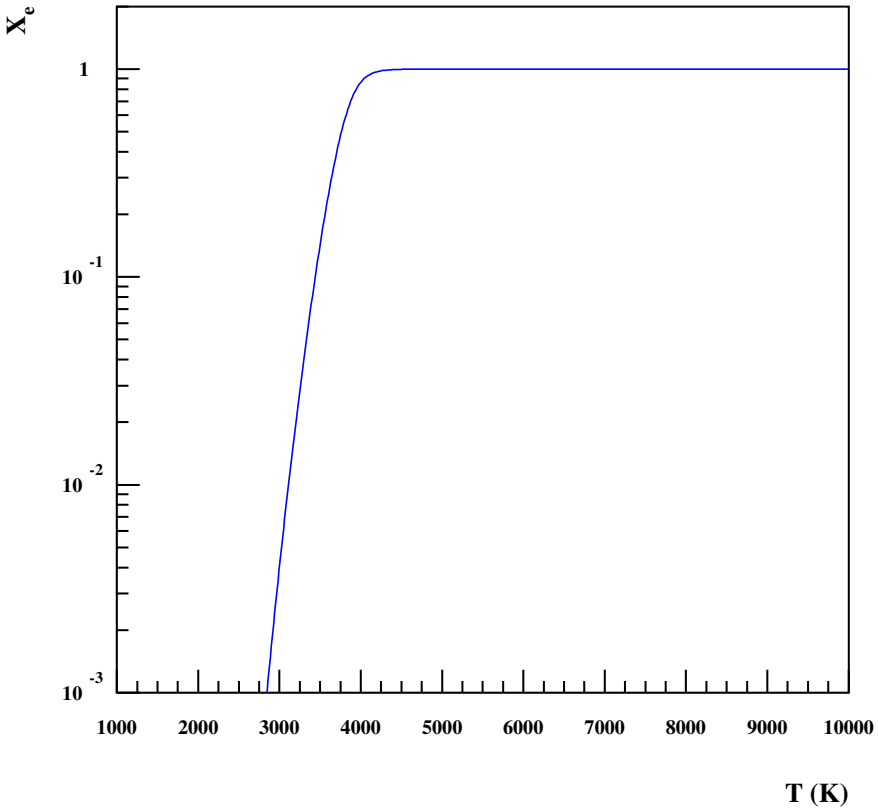

Figure 1: Number of free electrons per baryon X_e as a function of the temperature of the universe.

which corresponds to a flat (i.e. Euclidean) space. It is given by :

$$\rho_{0,C} = \frac{3H_0^2}{8\pi G} = 1.88\, h^2 \times 10^{-29}\ \mathrm{g/cm^3} \text{ or } 2.9\, h^2 \times 10^{11}\ \mathrm{M_\odot/Mpc^3} \tag{2.3}$$

where G is the gravitational constant. It corresponds to a density of a few hydrogen atoms per cubic meter or one typical galaxy per cubic megaparsec. Densities are usually given relative to $\rho_{0,C}$ with the notation $\Omega \equiv \rho/\rho_{0,C}$.

Table 1 gives the principal components to the density of the universe. The total density is very close to the critical density but is dominated by vacuum energy and dark matter contributions. The baryonic matter only amounts to ≈4% of the total density or 17% of the total matter content. What we can observe with our telescopes, because it emits light, corresponds to only $\sim 10^{-3}$ of the total. Nevertheless, in spite of its modest contribution, baryonic matter is important as this is the only one we know and observe. Is is usual to introduce η, the number of photon per baryon which remains constant during the expansion and is directly related to Ω_b by $\Omega_b{\cdot}h^2$=$3.65\times10^7\eta$. WMAP observations lead to $\Omega_b{\cdot}h^2$=$0.02249^{+0.00056}_{-0.00057}$ [9].

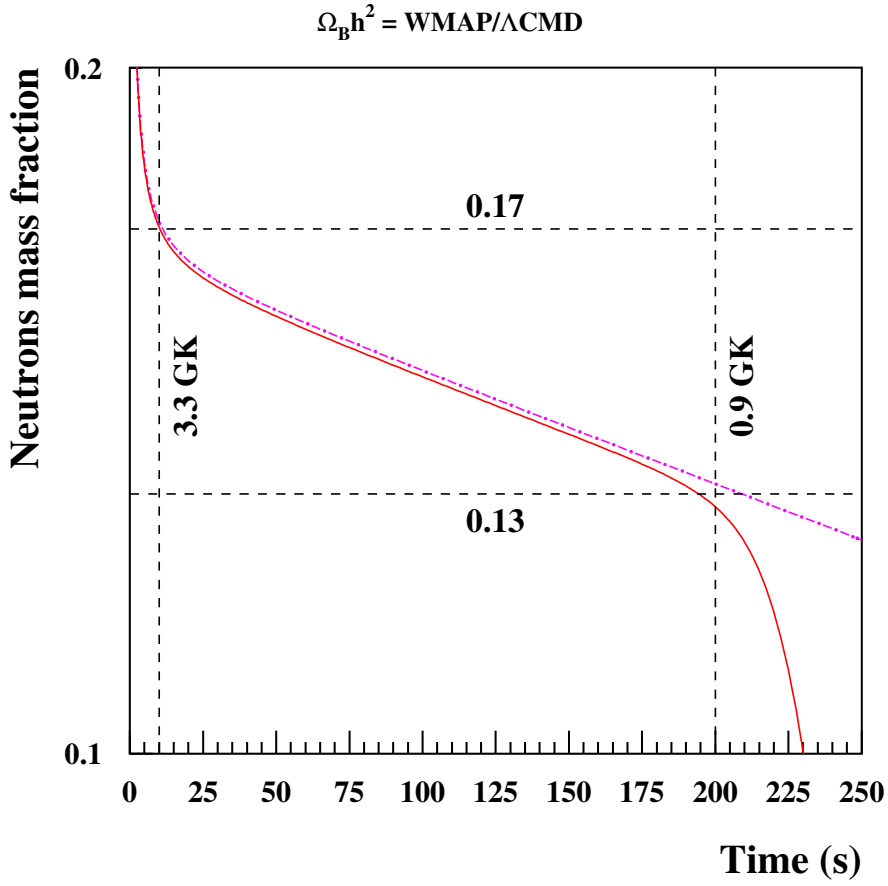

Figure 2: Neutron mass fraction as a function of temperature (log-lin scale). The curves represent the free neutron decay (dash–dotted line) and the full network calculation (solid line). Neutrons and protons remain in equilibrium until freezout at T = 10 to 3.3 GK and while nucleosynthesis begins below 0.9 GK and after $t \approx$3 mn.

2.2 Physics of the expanding Universe in the BBN era

At temperatures slightly above 10^{10} K, the particles present are: photons, electrons, positrons, the three families of neutrinos and antineutrinos plus a few neutrons and protons. The baryonic density does not have at this epoch any influence on the rate of expansion of the Universe (i.e. Hubble parameter). Its influence on nucleosynthesis is simply that a higher density of nuclei induces a larger number of reactions taking place between them per unit time.

All these particle are in thermal equilibrium so that, the numbers of neutrons and protons are simply related by $N_n/N_p = \exp(-Q_{np}/k_B T)$ where Q_{np} = 1.29 MeV is the neutron-proton mass difference. This holds until $T \lesssim 10^{10}$ K, when the weak rates that govern the n$\leftrightarrow$p reactions (ν_e+n$\leftrightarrow$e$^-$+p and $\bar{\nu}_e$+p$\leftrightarrow$e$^+$+n), become slower than the rate of expansion $H(t)$. Afterward, the ratio at *freezeout* $N_n/N_p \approx$0.17 further decreases to $N_n/N_p \approx$0.13 due to free neutron beta decay until the temperature is low enough ($T \approx 10^9$ K) for the first nuclear reaction n+p$\rightarrow$D+γ to become faster than the reverse photodisintegration (D+$\gamma\rightarrow$n+p) that up to now prevented the production of

heavier nuclei. Figure 2 shows that freezout is not instantaneous and that free neutron decay only occurs between 3.3 and 0.9 GK. From that point on, the remaining neutrons almost entirely end up bound in ^{4}He while only traces of D, ^{3}He and ^{7}Li are produced.

Hence, the ^{4}He yield is directly related to the N_n/N_p ratio at freezeout that is at the expansion rate $H(t)$ compared to the weak rates. $H(t)$ is obtained from the Einstein equation that links the curvature and energy–momentum tensors, associated with the metrics (Friedmann–Lemaître–Robertson–Walker),

$$ds^2 = dt^2 - a^2(t)\left(\frac{dr^2}{1-kr^2} + r^2(d\theta^2 + \sin\theta d\phi^2)\right) \tag{2.4}$$

which represents the *Cosmological Principle*: homogeneity and isotropy of the Universe. $a(t)$ is the above mentioned scale factor and $k = 0$ or ± 1 marks the absence or sign of space curvature. In an appropriate (free falling) reference frame, the energy–momentum tensor has only non-zero diagonal elements : (ρ, p, p, p) where ρ and p are the energy density and pressure of the fluid. It leads to the Friedmann equation that links the rate of expansion ($H(t) \equiv \dot{a}(t)/a(t)$) to the energy density ρ:

$$\left(\frac{\dot{a}}{a}\right)^2 + \frac{k}{a^2} = \frac{8\pi G\rho}{3} \tag{2.5}$$

(Setting $k = 0$ leads to the expression 2.3 of the critical density.) The equation can be conveniently re–written in term of the present day components of the matter–energy density (Table 1), Hubble parameter, and scale factor:

$$\left(\frac{\dot{a}}{a}\right)^2 = H_0^2\left[\Omega_M\left(\frac{a_0}{a}\right)^3 + \Omega_R\left(\frac{a_0}{a}\right)^4 + \Omega_\Lambda + (1-\Omega_T)\left(\frac{a_0}{a}\right)^2\right] \tag{2.6}$$

From this equation, it is straightforward to deduce the time evolution of the scale factor in the radiation ($a(t) \propto t^{\frac{1}{2}}$), matter ($a(t) \propto t^{\frac{2}{3}}$) and vacuum ($a(t) \propto \exp(H_0\Omega_\Lambda^{\frac{1}{2}}t)$) dominated eras, from which, the time evolutions of T ($\propto a^{-1}$, from constant entropy) and ρ_B ($\propto a^{-3}$) can be deduced. Equation 2.6 can be rewritten as:

$$H(z) = H_0\Omega^{\frac{1}{2}}(z) \tag{2.7}$$

with

$$\Omega(z) \equiv \Omega_M(z+1)^3 + \Omega_R(z+1)^4 + \Omega_\Lambda + (1-\Omega_T)(z+1)^2 \tag{2.8}$$

Given the values from see Table 1, at BBN when $z \sim 10^8$, the dominant term is the "radiation" term, Ω_R. This corresponds to all the relativistic particles whose energies also scale as a^{-1} in addition to the a^{-3} number density factor. The important consequence is that during BBN, $H(t)$ is only governed by relativistic particles while the baryons, cold dark matter, cosmological constant or curvature (k or $(1-\Omega_T)$) terms play no role. The rate of expansion is thus given by $H(t) = \sqrt{8\pi G\rho_R/3}$ with the radiation density, ρ_R, given by the Stefan-Boltzmann law:

$$\rho_R = g\frac{\mathrm{k}_B^2\pi^2}{30\hbar^3}T^4 \equiv \frac{g}{2}\mathrm{a}_R T^4 \quad \text{(bosons)} \tag{2.9}$$

where $g \equiv 2J+1$ is the spin factor and a_R the radiation constant. For fermions (e.g. electrons), an additional factor of 7/8 must be inserted. In the radiation dominated era, in particular during BBN,

the expansion rate is hence simply given by:

$$H \equiv \frac{\dot{a}}{a} = \sqrt{\frac{8\pi\, G\, a_R\, g_{eff}(T)}{6}} \times T^2 \tag{2.10}$$

The effective spin factor, g_{eff}, decreases whenever the temperature drops below a mass threshold for the particle–antiparticle annihilation of each species, so that during BBN, only e^+ and e^- annihilation has to be considered. Hence, the contributions to $g_{eff}(T)$ come from photons ($g \equiv 2$), neutrinos ($g = 2\times N_\nu \frac{7}{8}(T_\nu/T)^4$ as $T_\nu \neq T_\gamma$, with N_ν=3 the number of neutrino families) and electrons/positrons (from $2\times 2\times \frac{7}{8}$ for $T \gg m_e$ to 0 for $T \ll m_e$). When particles annihilate the released energy is shared among the other particles they were in equilibrium with. The weak rates decrease much faster ($\sim T^5$) than the expansion rate ($\sim T^2$) so that below $\approx 10^{10}$ K, neutrinos are not anymore in thermal equilibrium with electrons and positrons whose annihilations only re-heat the photon bath, not the neutrinos. The ratio of photon and neutrino temperatures T_γ/T_ν evolving between 1 and $(11/4)^{\frac{1}{3}} \approx 1.4$. Figure 3 displays the temperature and baryonic density as a function

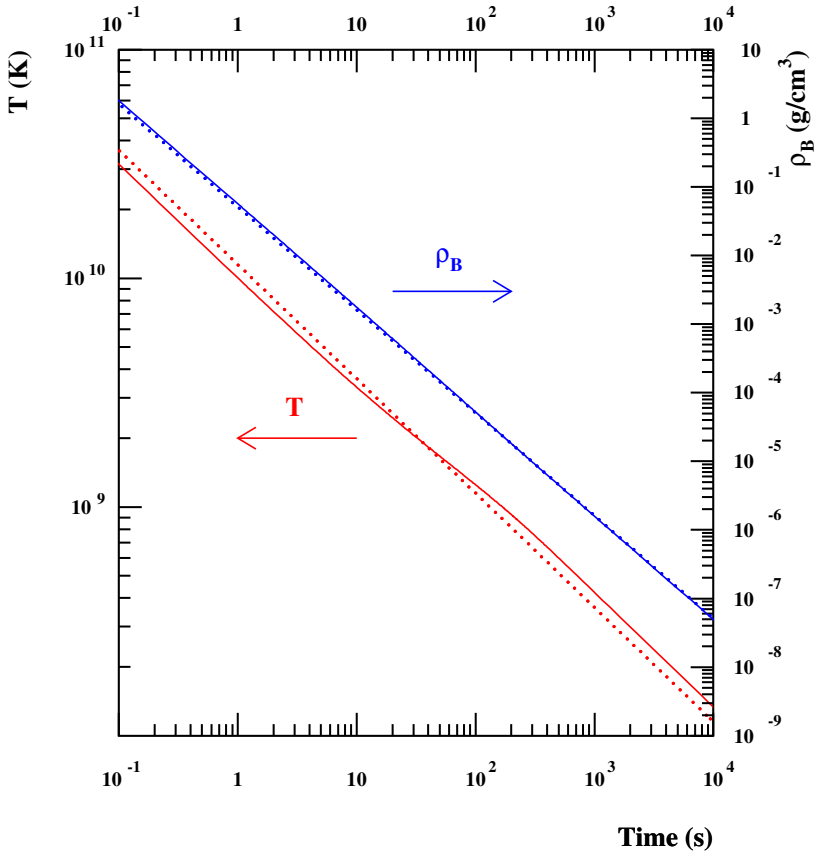

Figure 3: Baryonic density (right axis) and (photon) temperature (left axis) as a function of time. The dotted line correspond to $T \propto t^{-\frac{1}{2}}$ and $\rho_B \propto t^{-\frac{3}{2}}$ while the solid line the exact calculation showing the effect of re-heating by electron–positron annihilation.

of time: n↔p freezeout (at $T \approx 10^{10}$) and nucleosynthesis ($T < 10^9$) occur a densities of ≈0.1

and $\lesssim 10^{-5}$ g/cm^3. These densities are very small compared to those prevailing in stellar interiors preventing three body reactions like $3\alpha \rightarrow {}^{12}$C to be efficient.

In conclusion, the primordial ^{4}He abundance is directly related to the expansion rate governed by the relativistic particles, compared to the weak rate. It can hence be used to set constraints on physics beyond the Standard Model.

2.3 Primordial abundances

During the evolution of the Galaxy, nucleosynthesis takes place mainly in massive stars which release matter enriched in heavy elements into the interstellar medium when they explode as supernovae. Accordingly, the abundance of heavy elements, in star forming gas, increases with time. The observed abundance of *metals*[3] is hence an indication of its age: the older the lower the *metallicity*. Primordial abundances are hence extracted from observations of object with small metallicity, possibly followed by an extrapolation to zero metallicity.

Lithium, beryllium and boron can be observed at the surface of stars found in the halo of our galaxy. While the abundances of beryllium and boron increases with metallicity (i.e. with time) confirming that these elements are continuously synthesized [4], for [Fe/H] $<$ -1.3 the abundance of lithium is independent of metallicity, displaying a plateau. This was discovered by François and Monique Spite [10] who interpreted this constant Li abundance as corresponding to the BBN ^{7}Li production. This interpretation assumes that lithium has not been depleted at the surface of these stars so that the presently observed abundance is equal to the initial one. The presence of the thin "Spite plateau" is an indication that depletion may not have been very effective. On the contrary, younger stars ([Fe/H] $>$ -1) display a large dispersion in lithium abundances reflecting the effects of different production and destruction mechanisms. Recent observations [11] have led to a relative primordial abundance of Li/H = $(1.58 \pm 0.31) \times 10^{-10}$ [12], obtained by extrapolation to zero metallicity (Fe/H=0).

Contrary to ^{7}Li which can be both produced (spallation, AGB stars, novae) and destroyed (in the *interior* of stars), deuterium, a very fragile isotope, can only be destroyed after BBN, in particular at the very first stage of star formation. Its primordial abundance has thus to be determined from the observation of cold objects. Clouds at high redshift on the line of sight of even more distant quasars are thought to be the best candidates. Absorption line observations enable the determination of the D/H ratio. Unfortunately, there are few good candidates (half a dozen) : there is no evidence for a plateau nor of a tendency that could be extrapolated to zero metallicity. The adopted primordial D abundance is hence given by the average value $(2.82^{+0.20}_{-0.19}) \times 10^{-5}$ of D/H observations in these cosmological clouds [13].

After BBN, ^{4}He is only produced by stars. Its primordial abundance is deduced from observations in HII (ionized hydrogen) regions of compact blue galaxies. Galaxies are thought to be formed by the agglomeration of such dwarf galaxies which are hence considered as more primitive. The primordial ^{4}He abundance Y_p (^{4}He mass fraction) given by the extrapolation to zero

[3] In astrophysics, *metals* means all elements with $Z > 2$ and the abundance of metals is called *metallicity*. Logarithm of metallicity relative to solar ($\odot$) is often used with the notation [X/H]=log(X/H) $-$ log(X$_\odot$/H$_\odot$) where X is usually Fe. Hence, for instance, [Fe/H]=0 or -3 correspond to a solar, or 10^{-3} solar metallicity.

[4] Be, B, ^{6}Li and some ^{7}Li are produced by a *spallation* process: mainly breaking C, N and O nuclei by p and α at high energy in the interstellar medium.

metallicity of helium abundances is affected by systematic uncertainties. Here, we will use a safe interval $Y_p = 0.2534 \pm 0.0083$ [14].

Contrary to ^{4}He, ^{3}He is both produced and destroyed in stars so that the evolution of its abundance as a function of time is not well known. Because of the difficulties of helium observations and the small ^{3}He/^{4}He ratio, ^{3}He has only been observed in our galaxy. The ^{3}He abundances observed in galactic HII regions display a plateau as a function of the galactic radius and in a limited range of metallicities: -0.6 < [Fe/H] < 0.1 [15]. It is however difficult to extrapolate this galactic value (spanning only a limited range of Fe/H) to zero metallicity so that ^{3}He is not usually used to constrain BBN. An upper limit on ^{3}He primordial abundance is given by Bania et al. [15]: ^{3}He/H = $(1.1 \pm 0.2) \times 10^{-5}$, based on their best observed source.

2.4 Nuclear reactions

Unlike in other sectors of nuclear astrophysics, nuclear cross sections have usually been directly measured at BBN energies (∼100 keV). Table 2 lists the 12 nuclear reactions responsible for the production of ^{4}He, D, ^{3}He and ^{7}Li in Standard BBN. Note the presence of the radioactive tritium (^{3}H) and ^{7}Be that will later decay into ^{3}He and ^{7}Li respectively. There are many other reactions that connects these isotopes, but their cross sections are too small and/or reactants too scarce to have any significant effect. This Table presents the sensitivity of the calculated abundances (Y_i

Table 2: Abundance sensitivity: $\partial \log Y / \partial \log < \sigma v >$ at WMAP baryonic density.

Reaction	^{4}He	D	^{3}He	^{7}Li	$E_0(\Delta E_0/2)$ (MeV)
n↔p ($\propto 1/\tau_n$)	-0.73	0.42	0.15	0.40	
^{1}H(n,γ)^{2}H	0	-0.20	0.08	1.33	
^{2}H(p,γ)^{3}He	0	-0.32	0.37	0.57	0.11(0.11)
^{2}H(d,n)^{3}He	0	-0.54	0.21	0.69	0.12(0.12)
^{2}H(d,p)^{3}H	0	-0.46	-0.26	0.05	0.12(0.12)
^{3}H(d,n)^{4}He	0	0	-0.01	-0.02	0.13(0.12)
^{3}H(α,γ)^{7}Li	0	0	0	0.03	0.23(0.17)
^{3}He(n,p)^{3}H	0	0.02	-0.17	-0.27	
^{3}He(d,p)^{4}He	0	0.01	-0.75	-0.75	0.21(0.15)
^{3}He(α,γ)^{7}Be	0	0	0	0.97	0.37(0.21)
^{7}Li(p,α)^{4}He	0	0	0	-0.05	0.24(0.17)
^{7}Be(n,p)^{7}Li	0	0	0	-0.71	

with i = ^{4}He, D, ^{3}He and ^{7}Li) with respect to a change of each of the 12 reaction rates by a constant factor. We define the sensitivity as $\partial \log Y / \partial \log < \sigma v >$, calculated at the WMAP baryonic density:

$$\frac{\Delta Y}{Y} = \left.\frac{\partial \log Y}{\partial \log < \sigma v >}\right|_{WMAP} \times \frac{\Delta < \sigma v >}{< \sigma v >} \tag{2.11}$$

so that the impact of a change in a reaction rate on primordial abundances can be readily estimated. The last column represents the Gamow window at BBN typical temperatures. Figure 4 displays the

most important reactions for the BBN ^{4}He, D, ^{3}He and ^{7}Li production. The main reactions for the production of ^{6}Li, ^{10}B, ^{11}B and CNO (through ^{12}C) isotopes are also shown for completeness but their primordial abundances are smaller by orders of magnitude.

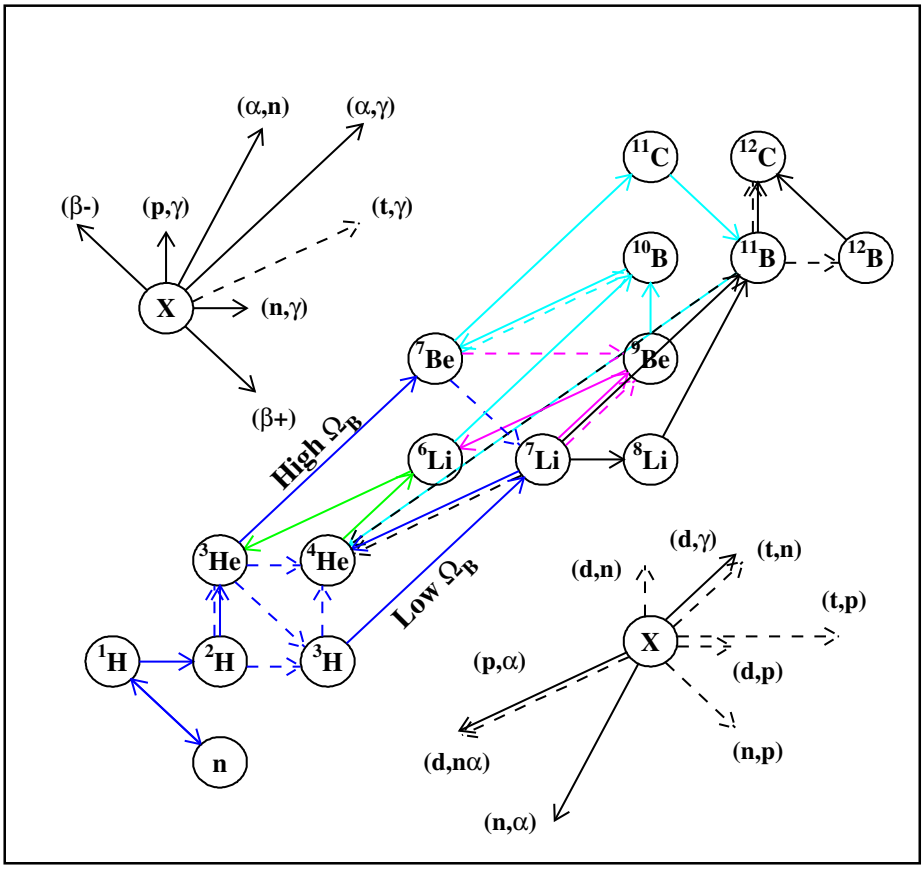

Figure 4: The BBN most important reactions for the productions of ^{4}He, D, ^{3}He and ^{7}Li, LiBeB and CNO isotopes.

The weak reactions involved in n↔p equilibrium are an exception; their rates come from the standard theory of the weak interaction. They are calculated with, as only experimental input, the neutron lifetime whose experimental value is still a matter of debate [8]. Until very recently, the averaged value of 885.7±0.8 s was recommended by the Particle Data Group, in spite of a new measurement that lead to a significantly different value of 878.5±0.7±0.3 [16]. Newer experimental results and analyses have not yet been able to solve this discrepancy but have motivated a

reevaluation of the recommended value: 881.5±1.5 s [17], awaiting experimental clarification. The n+p→D+γ reaction rate [18] is also obtained from theory but in the framework of Effective Field Theory. Few experimental data is available at BBN energies but they all confirm the theoretical results.

For the ten remaining reactions[5], ^{2}H(p,γ)^{3}He, ^{2}H(d,n)^{3}He, ^{2}H(d,p)^{3}H, ^{3}H(d,n)^{4}He, ^{3}H(α,γ)^{7}Li, ^{3}He(d,p)^{4}He, ^{3}He(n,p)^{3}H, ^{3}He(α,γ)^{7}Be, ^{7}Li(p,α)^{4}He and ^{7}Be(n,p)^{7}Li, cross sections have been measured in the laboratory at the relevant energies even though these experiments were in general motivated by nuclear physics rather than BBN studies. Compilations of experimental nuclear data to determine thermonuclear rates for astrophysics have been initiated by W. Fowler. This was later pursued within the European NACRE collaboration [19] which also provided upper and lower rate limits and more recently by Iliadis et al. [20] with an improved statistical treatment of uncertainties. For those reactions involved in BBN, the last two dedicated analyses were performed by Descouvemont et al. [21] and Cyburt [22]. In particular, in the former, all experimental data for the ten BBN reactions were compiled and analyzed in the framework of *R*–matrix theory for interpolation or extrapolation. In addition to providing more reliable recommended rate, the rate uncertainties were evaluated on statistical grounds [21]. We refer to these two most recent evaluations [21, 22] and to Serpico et al. [23] for extensive discussions of BBN reaction rates and their extraction from experimental data. Since these evaluations new experimental data has improved the accuracy and reliability of some of those reaction rates. As an example, Fig. 5 show for the ^{2}H(d,n)^{3}He reaction the available experimental data and the R–matrix fit [21] of the astrophysical *S*–factor [6]. Reference for the experimental data can be found in Descouvemont et al. [21] except for the new set of data from Leonard et al. [24], which is in agreement with the previous R–matrix results of 2004 within the BBN energy range (Table 2). Hence, these new data are important to confirm the previous results but have negligible effect on BBN results. On the contrary, since 2004, a wealth of new experimental data have been made available for the the important reaction ^{3}He(α,γ)^{7}Be (see Table 2). These are the results of several recent experiments that were motivated by the dispersion of previous experimental measurements, depending on the technique: "prompt" gamma-ray detection or ^{7}Be decay counting (i.e. "activation") methods. Cyburt and Davids [25] have re-evaluated this reaction rate in light of the new experimental data, obtaining a *S*–factor significantly higher than previously thought[7]. In addition, a new method has been used using a recoil separator to detect ^{7}Be ejectiles, together with the "prompt" and "activation" ones by Di Leva et al. [26]. Their results differ both in the absolute value and in the energy dependence of the cross section at energies higher than BBN. This stresses the need for further experimental and theoretical (energy dependence) efforts concerning this reaction.

2.5 BBN primordial abundances compared to observations

Figure 6 shows the evolutions of the abundances (in mass fraction) as a function of time at the WMAP (ΛCDM) baryonic density. (The sudden changes in the evolutions of the abundances as a

[5] We use here the usual nuclear physics notation A(x,y)B for the reaction A+x→B+y to recall that A, x, y an B were respectively the target nucleus, the ion beam, the detected particle and the recoil nucleus.

[6] The astrophysical *S*–factor is the cross section corrected for the strong effect of Coulomb barrier penetrability : $S(E) \equiv E\sigma(E)\exp(2\pi\eta)$ where, here, $\eta \equiv \frac{Z_p Z_c e^2}{\hbar v}$ is the Sommerfeld parameter.

[7] More precisely, $S(E=0)$ 13% higher than Descouvemont et al. [21]

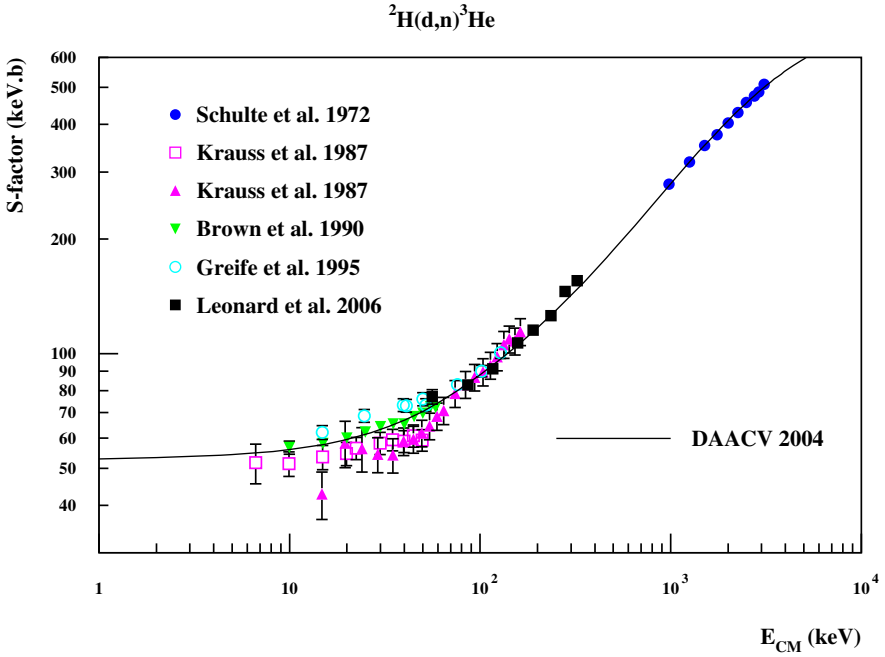

Figure 5: Experimental data for the, ^{2}H(d,n)^{3}He reaction, *S*–factor compared with the R–matrix fit of Descouvemont et al. [21]. (See this reference for reference to experimental data except for the more recent data from Leonard et al. [24].)

function of time, seen in the Figure, originate from successive departures from nuclear statistical or quasi–static equilibria [27, 28].) Neutrons are mostly captured to form ^{4}He while D and ^{3}He reach final values of $\approx 10^{-5}$. After a sharp rise, ^{7}Li is efficiently depleted by the ^{7}Li(p,α)^{4}He reaction. At this density, ^{7}Li is produced through the formation of ^{7}Be via the ^{3}He(α,γ)^{7}Be reaction. It will later decay to ^{7}Li. ^{7}Be destruction occurs through the ^{7}Be(n,p)^{7}Li(p,α)^{4}He channel which is limited by the scarcity of neutrons. At lower baryonic density more neutrons would survive but the ^{7}Li(p,α)^{4}He destruction mechanism would be less effective and ^{7}Li would be produced directly via the ^{3}H(α,γ)^{7}Li (Fig. 4). In Figure 7 is represented the abundances of ^{4}He (mass fraction), D, ^{3}He and ^{7}Li (in number of atoms relative to H) as a function of the baryonic density. The "U" shape of the ^{7}Li abundance curve comes from the two modes of ^{7}Li synthesis discussed above and shown on Figure 4. The thickness of the curves reflect the nuclear uncertainties. They were obtained [29, 30] by a Monte–Carlo calculation using for the nuclear rate uncertainties those obtained by [21] but with the new ^{3}He(α,γ)^{7}Be rate [25]. The horizontal lines represent the limits on the ^{4}He, D and ^{7}Li primordial abundances deduced from observations as discussed in § 2.3. The vertical stripe represents the baryonic density deduced from CMB observations by [9]. The primordial abundances (CMB+BBN) corresponding to this range of density are given in Table 3.

As shown on Figure 7, the primordial abundances deduced either by BBN at CMB deduced baryonic density or from observations are in perfect agreement for deuterium. Considering the large uncertainty associated with ^{4}He observations, the agreement with CMB+BBN is fair, but close to the lower limit. The calculated ^{3}He value is close to its galactic value showing that its abundance

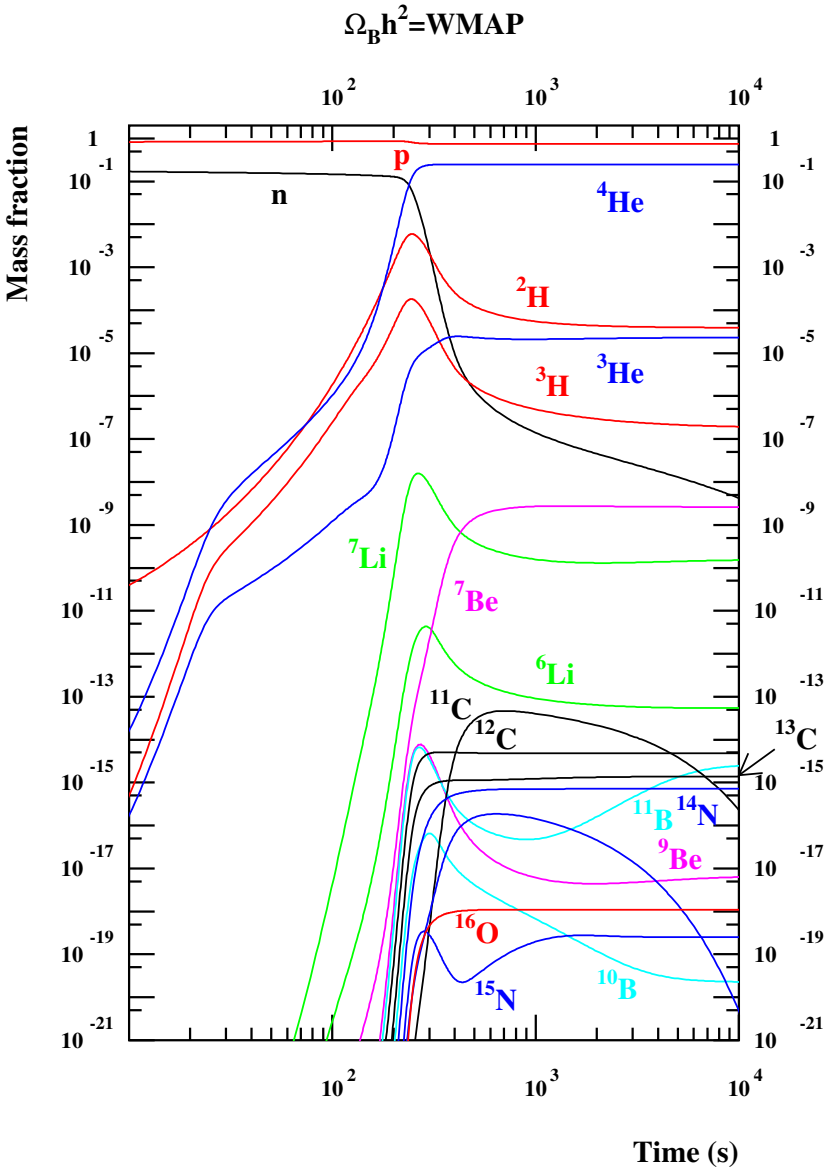

Figure 6: Evolution of the abundances as a function of time at WMAP baryonic density. For A>7, only selected isotopes are displayed.

has little changed during galactic chemical evolution. On the contrary, the ^{7}Li, CMB+BBN, calculated abundance is significantly higher (a factor of ≈3–4) than the primordial abundance deduced by [11]. The origin of this discrepancy between CMB+BBN and spectroscopic observations remains an open question. Indeed, it seems surprising that the major discrepancy affects ^{7}Li since it could a priori lead to a more reliable primordial value than deuterium, because of much higher observational statistics and an easier extrapolation to primordial values (see Fig. 2 and 3 in [1]). There are many tentative solutions to this problem (nuclear, observational, stellar, cosmological,...)

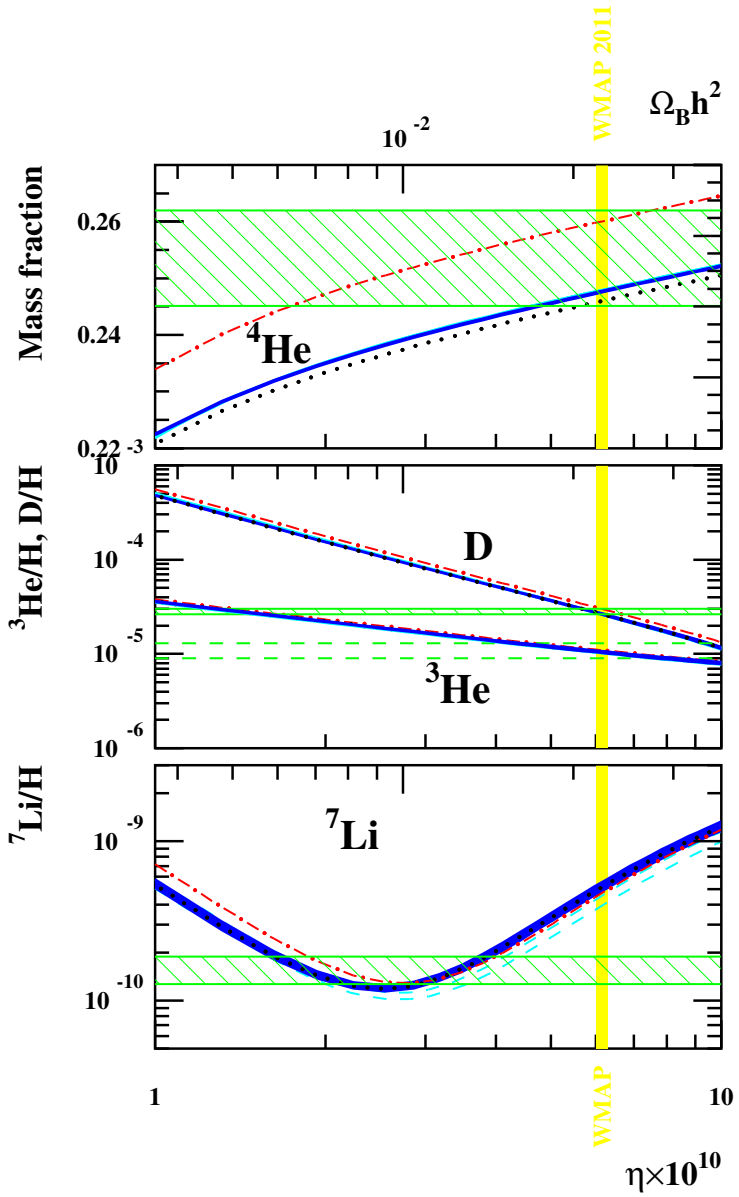

Figure 7: Abundances of ^{4}He (mass fraction), D, ^{3}He and ^{7}Li (by number relative to H) as a function of the baryon over photon ratio η (or $\Omega_b \cdot h^2$.) showing the effect of nuclear uncertainties. The vertical stripe corresponds to the WMAP baryonic density [9] while the horizontal area represent the primordial abundances. The dashed curves represent previous calculations [29] before the re-evaluation [25] of the ^{3}He$(\alpha,\gamma)^7$Be rate. The dotted and dot-dashed lines corresponds, respectively, to the alternative value [16] of the neutron lifetime and to 4 *effective* neutrino families.

Table 3: Yields at WMAP baryonic density.

	Cyburt el al 2008[31]	CV10[30]	Observations	Factor
^{4}He	0.2486±0.0002	0.2476±0.0004	0.2534±0.0083 [14]	$\times 10^0$
D/H	2.49±0.17	2.68±0.15	$2.82^{+0.20}_{-0.19}$ [13]	$\times 10^{-5}$
^{3}He/H	1.00±0.07	1.05±0.04	(0.9–1.3)[15]	$\times 10^{-5}$
^{7}Li/H	$5.24^{+0.71}_{-0.67}$	5.14±0.50	1.58±0.31 [12]	$\times 10^{-10}$

but none has provided yet a fully satisfactory solution. The derivation of the lithium abundance in halo stars with the high precision needed is difficult and requires a fine knowledge of the physics of stellar atmosphere (effective temperature scale, population of different ionisation states, non Local Thermodynamic Equilibrium effects and 1D/3D model atmospheres). There is no lack of phenomena to modify the surface abundance of lithium: nuclear burning, rotational induced mixing, atomic diffusion, turbulent mixing, mass loss,.... One also notes that between the BBN epoch and the birth of the now observed halo stars, ≈1 Gyr has passed. Primordial abundances could have been altered during this period. However, the flatness of the plateau over three decades in metallicity and the relatively small dispersion of data represent a real challenge to stellar modeling [32]. In the nuclear sector, large systematic errors on the 12 main nuclear cross sections are excluded. Since the CMB results point toward the high η region, a peculiar attention should be paid to ^{7}Be nucleosynthesis. However, there is no indication that a more efficient ^{7}Be nuclear destruction mechanism be at work. Nuclear mechanisms to destroy this ^{7}Be have been explored [29, 33, 34]. An increased ^{7}Be(d,p)2α cross section has been proposed but was not confirmed by experiments [35, 36, 37]. Other ^{7}Be destruction channels have recently been proposed and await experimental investigation. Another scenario would be to take advantage of an increased late time neutron abundance. This is exactly what happens (in the context of varying constants) when the ^{1}H(n,γ)^{2}H rate is decreased. The neutron late time abundance is increased (with no effect on ^{4}He) so that more ^{7}Be is destroyed by ^{7}Be(n,p)^{7}Li(p,α)α, (see Fig. 1 in [38]). Figure 7 also displays the effect of using a different value of the neutron lifetime (878.5 s [16] instead of 885.7) or an *effective* number of neutrino families of 4. In both cases, it shifts the temperature at freezeout (§ 2.2), essentially affecting the ^{4}He primordial abundance without sufficient impact on ^{7}Li. (See also T. Kajino's lecture for particle physics proposed solutions.)

The primordial abundances of ^{6}Li, ^{9}Be, ^{10}B and ^{11}B (in number of atoms relative to H) can be deduced from mass fractions[8] in Figure 6: 1.3×10^{-14} (see [39]), 1×10^{-18}, 3×10^{-21}, and 3×10^{-16} [40]. These are orders of magnitudes lower than present–day observations of very low metallicity stars, even for ^{6}Li, for which the existence of a plateau, in the ^{6}Li/H, 10^{-12} to 10^{-11} range, is debated [41, 32]. During BBN, ^{6}Li is produced by the D(α,γ)^{6}Li and destroyed by ^{6}Li(p,α)^{3}He reactions (see Fig. 4), both of which rates are now established [19, 39]. The BBN, CNO production (mostly ^{12}C) is too small (CNO/H≈7×10^{-16}) to affect the evolution of the first massive stars, by

[8]The number of atom of isotope i per unit volume N_i is related to the mass fraction X_i by $N_i = X_i \mathrm{N}_A \rho / \mathrm{A}_i$, where N_A, and A_i are respectively the Avogadro's number and the atomic mass number. The number of atoms relative to H is just $N_i/N_\mathrm{H} \equiv X_i/X_\mathrm{H}\mathrm{A}_i$ with $X_\mathrm{H} \approx 0.75$.

promptly triggering the CNO cycle, even considering the nuclear uncertainties [40]. It is worth noting that CNO production was found to be sensitive to the ^{7}Li(d,n)2^{4}He reaction rate. Not so much because it is a minor source of uncertainty but because this effect is unexpected. The explanation is that even though the ^{4}He, D, ^{3}He and ^{7}Li *final abundances are left unchanged*, the peak ^{7}Li abundance at $t \approx$200 s (Fig. 6) is reduced by a factor of about 100, an evolution followed by ^{8}Li and CNO isotopes.

2.6 BBN as a probe of the early Universe

Now that the baryonic density of the Universe has been deduced from the observations of the anisotropies of the CMB radiation with a precision that cannot be matched by BBN, one may wonder whether primordial nucleosynthesis studies are still useful.

The CMB radiation that is observed was emitted when the Universe became transparent $\approx 3 \times 10^5$ years after the Big-Bang. On the contrary, the freezeout of weak interactions between neutrons and protons, and BBN, occurred at a fraction of a second, and a few minutes after the Big–Bang. With the exception of the baryonic density, BBN parameters have *all been determined by laboratory measurements*. Hence, comparison between light–element observed and calculated abundances can be used to constrain the physics prevailing in the first seconds or minutes of the Universe.

Figure 7 shows the effect of an increase of the expansion rate of the Universe (see § 2.2), by assuming an *effective* number of neutrino families of 4 instead of 3. In fact a 10% change in the expansion rate would be sufficient to drive the ^{4}He and D abundances out of the observational limits while it provides little help to the ^{7}Li discrepancy. ^{4}He yield is sensitive to the value of the expansion rate at the time of n/p freezeout, i.e., around 10^{10} K and 0.1 to 1 s after the Big Bang while the other isotopes are sensitive to its value 3 to 20 mn after. There are several potential sources of deviations from the nominal expansion rate $H(t)$ as it can be seen from the examination of equation 2.10, for instance a modification of gravity, affecting G, or new particles, affecting $g_{eff}(T)$. (See T. Kajino's lecture for detailed example of Non-Standard Big–Bang Nucleosynthesis.)

3. Variation of constants and nuclear physics

Experimental (or observational) tests of variations of a constant consists in comparing quantities that have a different sensitivity to this constant (for reviews, see [5, 6]). Tests involve atomic clocks, atomic absorption in quasar (QSO) spectra, the CMB, and nuclear physics (Big Bang Nucleosynthesis, the triple–alpha reaction and stellar evolution, radioactivities in meteorites and the Oklo fossil reactor). They are all interesting because they have different dependency to the variation of constants and they probe variations on different cosmic time scale (Fig. 8). The frequencies of atomic fine versus hyperfine transitions, or of atomic lines of different elements have different dependency on the fine structure constant. The comparison between laboratory clocks or QSO absorption lines at high redshift provide constraints on the variation of α_{em} at different epochs (Fig. 8). In the following, we consider only those related to nuclear physics, and in particular the triple–alpha reaction in stars, and BBN. We will illustrate the effect of varying "constants" as the fine structure constant, the Fermi constant, the electron mass, ... on some nuclear reactions or decay but leave aside the discussion of the *coupled* variations of these constants which are beyond

the scope of this school. Indeed, within theories like superstring theory, the constants cannot be treated independently: their variations are related to each other in a way that depend on the model.

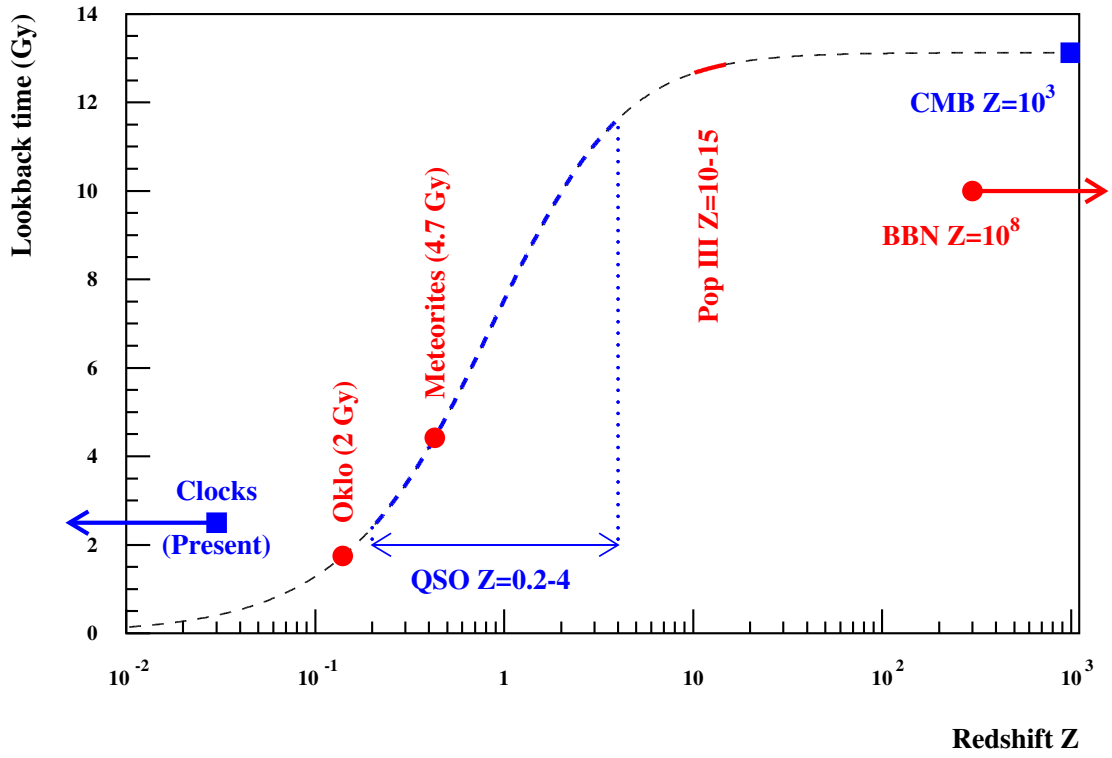

Figure 8: Test of the variations of constants performed at different redshifts or lookback time (i.e. elapsed time until present).

3.1 Variation of constants and the triple–alpha reaction

The ^{4}He$(\alpha\alpha,\gamma)^{12}$C reaction is very sensitive to the position of the "Hoyle state". The corresponding resonance width is very small (a few $\sim$eV) as compared with the competing reaction ^{12}C$(\alpha,\gamma)^{16}$O, dominated by broad ($\sim$100 keV) resonances and subthreshold levels. In Fig. 9, we show the low energy level schemes of the nuclei participating to the ^{4}He$(\alpha\alpha,\gamma)^{12}$C reaction: ^{4}He, ^{8}Be and ^{12}C. The triple-α reaction begins when two alpha particles fuse to produce a ^{8}Be nucleus whose lifetime is only $\sim 10^{-16}$ s but is sufficiently long so as to allow for a second alpha capture into the second excited level of ^{12}C, at 7.65 MeV above the ground state. This excited state of ^{12}C corresponds to an $\ell = 0$ resonance, as postulated by Hoyle [42] in order to increase the cross section during the helium burning phase. This "Hoyle state" decays to the first excited level of ^{12}C at 4.44 MeV through an $E2$ (i.e. electric with $\ell = 2$ multipolarity) radiative transition as the transition to the ground state ($0^+_1 \rightarrow 0^+_2$) is suppressed (pair emission only).

Assuming *i*) thermal equilibrium between the ^{4}He and ^{8}Be nuclei, so that their abundances are related by the Saha equation and *ii*) the sharp resonance approximation for the alpha capture on

^{8}Be, the ^{4}He$(\alpha\alpha,\gamma)^{12}$C rate can be expressed [43] as:

$$N_A^2\langle\sigma v\rangle^{\alpha\alpha\alpha} = 3^{3/2}6N_A^2\left(\frac{2\pi}{M_\alpha k_B T}\right)^3\hbar^5\omega\gamma\exp\left(\frac{-Q_{\alpha\alpha\alpha}}{k_B T}\right) \tag{3.1}$$

with $\omega\gamma \approx \Gamma_\gamma(^{12}\mathrm{C})$, the radiative partial width of the Hoyle level and $Q_{\alpha\alpha\alpha}$ =380 keV its energy relative to the triple alpha threshold. The variation of $Q_{\alpha\alpha\alpha}$ with the nucleon nucleon interaction dominates the variation of the reaction rate in Eq. (3.1). However, a more accurate calculation requires a numerical integration, as done in [19], to take into account *i*) the two step process, two alpha particle fusion into the ^{8}Be ground state at a resonance energy of $E_R(^8\mathrm{Be})$ followed by another alpha capture to the Hoyle state at a resonance energy of $E_R(^{12}\mathrm{C})$ [$Q_{\alpha\alpha\alpha} \equiv E_R(^8\mathrm{Be})+E_R(^{12}\mathrm{C})$] and *ii*) the energy dependent finite widths of those two resonances. Both the ^{8}Be ground state and the ^{12}C "Hoyle state" are known to be well described within a 2– or 3–alpha–particle cluster model, from which the dependence of the level energies to an effective nucleon–nucleon interaction can be obtained. This, in turn, can be related to more fundamental parameters to constrain the values of the fine structure and strong coupling constants. Small variations of the NN–interaction induce huge variations (many orders of magnitudes) on the triple–α reaction rate. This effect was investigated for 1.3, 5, 15, 20 and 25 $M_\odot$ stars with solar metallicity (Population I) [44, 45] and it was estimated that outside a window of 0.5% and 4% for the values of the strong and electromagnetic forces respectively, the stellar production of carbon or oxygen will be reduced by a factor 30 to 1000. This concerned stars born a few Gy ago, at redshift $z < 1$. Considering instead (see [46] for more details) the very first generation of stars (Population III) extends the test to a much larger lookback time. These stars are thought to have been formed a few 10^8 years after the Big Bang, at a redshift of $z \sim 10-15$, and with *zero initial metallicity*. For the time being, there are no direct observations of those Population III stars but one may expect that their chemical imprints could be observed indirectly in the most metal-poor halo stars (Population II). Depending on the NN–interaction, helium burning results in a stellar core with a very different composition from pure ^{12}C to pure ^{16}O (and even pure ^{24}Mg), due to the competition between the ^{4}He$(\alpha\alpha,\gamma)^{12}$C and ^{12}C$(\alpha,\gamma)^{16}$O reaction. As both C and O are observed in metal-poor halo stars, a ^{12}C/^{16}O abundance ratio close to unity is required. To be achieved, the NN–interaction should not have changed by more than $\sim 10^{-3}$, which can be translated in limits on $\Delta\alpha_{\mathrm{em}}$ [46].

3.2 Variation of constants and BBN

We have mentioned in § 2.6 that, at the BBN epoch, gravity could be different from General Relativity as in superstring theories. That would affect the rate of expansion, through G in equation 2.10. Here, we will illustrate the influence of the variations of constants on two key nuclear reaction rates : n↔p and n+p→d+γ. The first, together with the expansion rate, governs the production of ^{4}He, while the second triggers further nucleosynthesis. The weak rates that exchange protons with neutrons can be calculated theoretically and their dependence on G_F (the Fermi constant), Q_{np} (the neutron–proton mass difference) and m_e (the electron mass) is explicit. For instance, in laboratory conditions, the $n \to p + e^- + \bar{\nu}_e$, neutron free decay rate is well approximated by:

$$\tau_n^{-1} = \frac{1}{60}\frac{1+3\,g_A^2}{2\pi^3}G_F^2\,m_e^5\left(\sqrt{q^2-1}(2q^4-9q^2-8)+15\ln(q+\sqrt{q^2-1})\right) \tag{3.2}$$

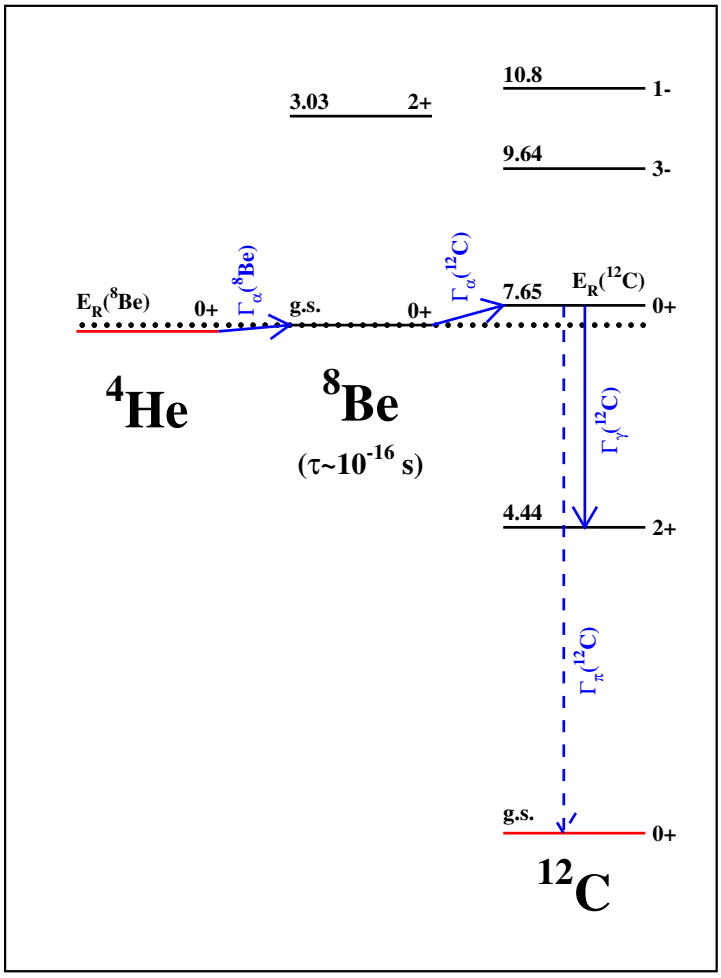

Figure 9: Level scheme showing the key levels in the triple α process.

which displays its G_F, $q \equiv Q_{np}/m_e$ and m_e explicit dependence. During BBN, the Fermi distributions of electrons, neutrinos and their antiparticles must be considered [47] but the explicit dependence remains. Figure 10 shows the dependence of the ^{4}He, D, ^{3}He and ^{7}Li, primordial abundances as a function of these three quantities, through the effect of the modified n$\leftrightarrow$p rates. The dependence of the n+p$\rightarrow$d+γ rate [18] cannot be explicitly related to a few fundamental quantities as for the weak rates but a modelisation of its dependence on the binding energy of deuteron B_D has been proposed [48]. Figure 10 shows that a variation of B_D (i.e. the n+p$\rightarrow$d+γ rate) has a strong influence on ^{7}Li, even reconciliating calculations with observations (see § 2.5). However, this is at

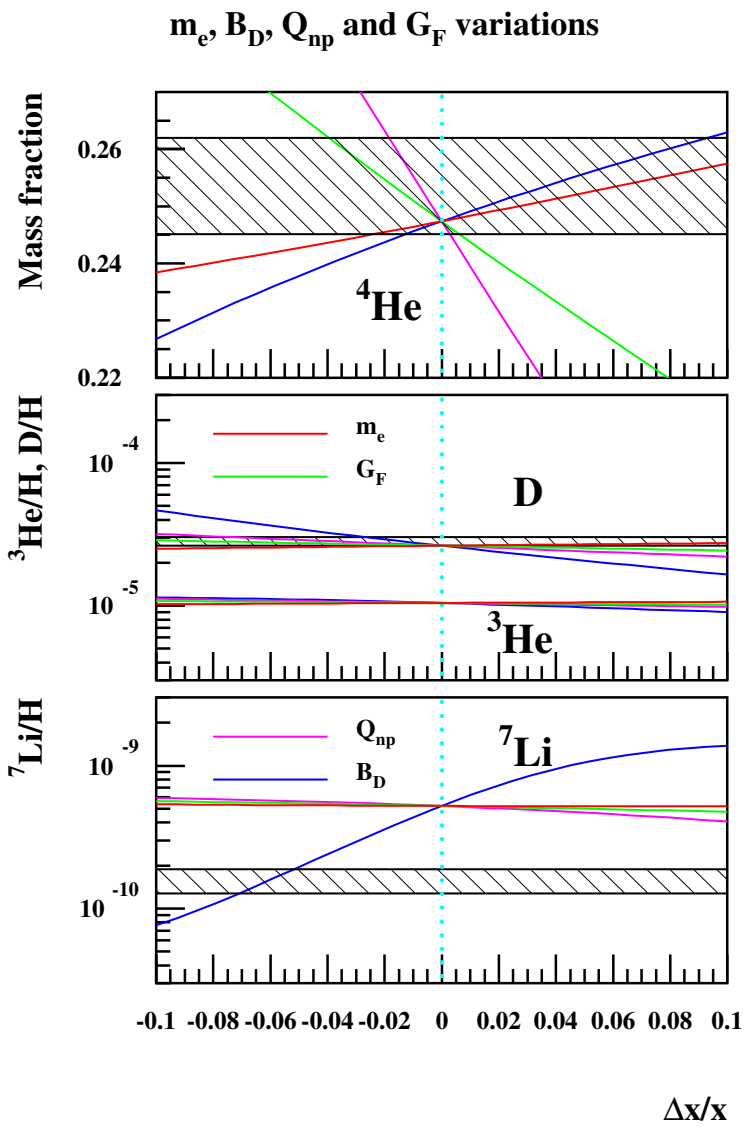

Figure 10: Abundances of ^{4}He (mass fraction), D, ^{3}He and ^{7}Li as a function of a change in the electron mass, the binding energy of deuterium, the neutron–proton mass difference, and the Fermi constant.

the expense of the agreement with ^{4}He, that could however be restored through the variation of the other quantities in Fig. 10 [38].

3.3 Other tests involving nuclear physics

Here, we briefly describe other constraints on the variations of constants given by nuclear physics and we refer to reviews [5, 6] and reference therein for details.

3.3.1 Meteorites and ^{187}Re

The ^{187}Re isotope is of special interest for the study of possible variation of constants [49, 5, 50] because of its very long lifetime, larger than the age of the Universe, and because of the high sensitivity of its lifetime to the variation of constants. It is the most abundant (62.6%) terrestrial rhenium isotope which $\beta+$ decays to ^{187}Os with a laboratory measured mean life of $\lambda_{\rm Lab}^{-1} = 61.0\times10^9$ years. Its $\beta+$ decay rate can be approximated by $\lambda \propto G_F^2 Q_\beta^3 m_e^2$ so that the the variation of λ can be related to a variation of the fine structure constant, using the liquid drop model to calculate the variation of the Coulomb energies of the parent and daughter nuclei:

$$\frac{\Delta\lambda}{\lambda} = 3\frac{\Delta Q_\beta}{Q_\beta} = \frac{3}{Q_\beta}\frac{(Z+1)^2 - Z^2}{A^{\frac{1}{3}}} a_C \frac{\Delta\alpha_{\rm em}}{\alpha_{\rm em}} \tag{3.3}$$

Thanks to the very low value of $Q_\beta = 2.66$ keV, the sensitivity is high: $\Delta\lambda/\lambda \approx 2\times10^4 \Delta\alpha_{\rm em}/\alpha_{\rm em}$[9]. The imprint or ^{187}Re decay since the birth of the Solar System can be found in the isotopic composition of some meteorites. Indeed, one has:

$$^{187}{\rm Re}\big|_{\rm Now} = {}^{187}{\rm Re}\big|_{\rm Init} \exp\left(-\bar{\lambda} t_{\rm M}\right) \tag{3.4}$$

$$^{187}{\rm Os}\big|_{\rm Now} = {}^{187}{\rm Os}\big|_{\rm Init} + {}^{187}{\rm Re}\big|_{\rm Init} \left[1 - \exp\left(-\bar{\lambda} t_{\rm M}\right)\right] \tag{3.5}$$

where $t_{\rm M}$ is the age of the meteorite ($\approx$ the age of the Solar System) and $\bar{\lambda}$ is the *averaged* ^{187}Re decay constant assuming that λ may have evolved over $\approx 4.6\times10^9$. It can be rewritten as:

$$^{187}{\rm Os}\big|_{\rm Now} = {}^{187}{\rm Os}\big|_{\rm Init} + {}^{187}{\rm Re}\big|_{\rm Now} \left[\exp\left(\bar{\lambda} t_{\rm M}\right) - 1\right] \tag{3.6}$$

which shows that the present day ^{187}Os versus ^{187}Re meteoritic isotopic abundances (relative to stable ^{188}Os) follow a linear dependence (an isochrone, see M. Gounelle lecture in this school) from which $\left[\exp\left(\bar{\lambda} t_{\rm M}\right) - 1\right]$ can be extracted. If the age of the meteorites $t_{\rm M}$ can be obtained by an other datation method (U/Pb isotopes) which is much less sensitive to the variation of $\alpha_{\rm em}$, then $\bar{\lambda}$ can be deduced and limits on $\Delta\alpha_{\rm em}$ can be obtained from those on $\bar{\lambda} - \lambda_{\rm Lab}$. In this illustrative example, we have only considered the effect of varying $\alpha_{\rm em}$ on the Coulomb contribution, but in theories that allows for variations of constants, $\alpha_{\rm QCD}$ should vary accordingly, inducing an exponentially larger variations of $\Lambda_{\rm QCD}$. The limits on $\Delta\alpha_{\rm em}$ would then be tighter but more model dependent. Letting aside the particle physics sector of coupled varying constants, in the nuclear physics sector it is not yet possible to relate explicitly Q_β to $\Lambda_{\rm QCD}$, so that approximations followed by scaling laws have to be used. This is a limitation for the use of nuclear constraints on the variation of constants beyond the simple cases like the n$\leftrightarrow$p equilibrium in BBN, as discussed above.

3.3.2 The Oklo nuclear fossil reactor

At present, terrestrial uranium is mainly composed of ^{238}U, 0.72% of ^{235}U and 0.0055% of ^{234}U. The ^{235}U isotope has a half–life of 7.038×10^8 years and decays by alpha emission. It is fissile through the absorption of thermal neutron that can lead, within special conditions, to the controlled chain reaction at work in nuclear reactors. One of the condition is that uranium be enriched in ^{235}U

[9] $a_C = 0.717$ MeV and Z = 75

to a level of 3–4%, another is that fission–produced neutrons are slowed down ("moderated") to take advantage of higher induced–fission cross–section. In 1972, the french Commissariat à l'Énergie Atomique discovered, in an uranium mine located at Oklo, in Gabon, that a *fossil, natural* nuclear reactor had been operating two billion years ago, during approximately a million years (see [51] and references therein). This operation was made possible because, at a few ^{235}U half–lives ago, its fractional abundance was sufficiently high, and hydrothermal water acted as moderator. As a result, the ore displayed a depletion in ^{235}U that was consumed by the chain reaction, and very peculiar isotopic rare-earth abundances. In particular ^{149}Sm (samarium) was strongly depleted, an effect ascribed to thermal neutron absorption through the $E_R = 0.0973$ eV resonance in ^{149}Sm(n,γ)^{150}Sm. As the neutron exposure time and energy distribution can be inferred from other rare-earth isotopic compositions, the samarium isotopic ratios are sensitive to ^{149}Sm(n,γ)^{150}Sm cross–section and hence on the position of the resonance. If its energy can be related to $\alpha_{\rm em}$ and other constants, in a manner similar as for ^{187}Re Q_β, new constraints can be obtained (see [5] and references therein).

4. Conclusions

The baryonic density of the Universe as determined by the analysis of the Cosmic Microwave Background anisotropies is in very good agreement with Standard Big–Bang Nucleosynthesis compared to D primordial abundance deduced from cosmological cloud observations. However, it disagrees with lithium observations in halo stars (Spite plateau). Presently, the most favored explanation is lithium stellar depletion but investigations of other solutions continue. The ^{6}Li abundance observed in halo stars cannot be explained by Standard Big–Bang Nucleosynthesis.

However, we stress here the importance of sensitivity studies in nuclear astrophysics: even in the simpler context of BBN without the complexity (e.g. mixing) of stellar nucleosynthesis, it would have been very unlikely to predict the influence of the ^{1}H(n,γ)^{2}H reaction on ^{7}Li nor of the ^{7}Li(d,n)2^{4}He reaction on CNO.

Nevertheless, primordial nucleosynthesis remains a invaluable tool for probing the physics of the early Universe. When we look back in time, it is the ultimate process for which we *a priori* know all the physics involved. Hence, departure from its predictions provide hints for new physics or astrophysics. Important issues in cosmology are modified gravity and varying constants.

In this last domain, nuclear physics can help setting constraints on the variation of fundamental constants over a wide range of cosmological time from BBN to near present.

Acknowledgments

I am indebted to all my collaborators on these topics, and in particular to Pierre Descouvemont, Keith Olive, Jean-Philippe Uzan and Elisabeth Vangioni.

References

[1] A. Coc, Third European School on Experimental Nuclear Astrophysics, Santa Tecla, 2–9 October 2005, EAS publications series, EDP Sciences, Vol. 27 pp. 41–52 (2007).

[2] K.A. Olive, CERN Yellow Report CERN-2010-002, pp.149-196; arXiv:1005.3955v1 [hep-ph].

[3] S. Weinberg, *Cosmology*, Oxford University Press, 2008, ISBN 978-0-19-852682-7.

[4] P. Peter & J.-Ph. Uzan, *Primordial Cosmology*, Oxford University Press, 2009, ISBN 978-0-19-920991.

[5] J.-Ph. Uzan, *Rev. Mod. Phys.*, **75** (2003) 403 [ArXiv:hep-ph/0205340]; *Living Rev. Relativity*, **14** (2011) 2 [arXiv:1009.5514].

[6] E. García–Berro, J. Isern and Y. A. Kubyshin, *Astron. Astrophys. Rev.*, **14** (2007) 113.

[7] The ALEPH Collaboration and The DELPHI Collaboration and the L3 Collaboration and The OPAL collaboration and The SLD Collaboration and the LEP Electroweak Working Group and the SLD Electroweak and Heavy Flavour Groups, *Phys. Rev.*, **427** (2006) 257.

[8] F.E. Wietfeldt and G.L. Greene, *Rev. Mod. Phys.*, **83** (2011) 1173.

[9] E. Komatsu, K.M. Smith, J. Dunkley et al., *Astrophys. J. S.*, **192** (2011) 18.

[10] F. Spite & M. Spite, *Astron. Astrophys.*, **115** (1982) 357.

[11] S.G. Ryan, T.C. Beers, K.A. Olive, B.D. Fields & J.E. Norris, *Astrophys. J.*, **530** (2000) L57.

[12] L. Sbordone, P. Bonifacio, E. Caffau et al., *Astron. Astrophys.*, **522** (2010) 26.

[13] M. Pettini, B.J. Zych, M. Murphy, A. Lewis and C.C. Steidel, *Mon. Not. R. Astron. Soc.*, **391** (2008) 1499.

[14] E. Aver, K.A. Olive and E.D. Skillman, arXiv:1112.3713, submitted to *JCAP*.

[15] T. Bania, R. Rood and D. Balser, *Nature*, **415** (2002) 54.

[16] A. Serebrov, V. Varlamova, A. Kharitonov et al., *Phys. Lett.*, **B605** (2005) 72.

[17] K. Nakamura et al. (Particle Data Group), *J. Phys.*, **G37** (2010) 075021, and 2011 partial update for the 2012 edition, http://pdg.web.cern.ch/pdg/.

[18] S. Ando, R.H. Cyburt, S.W. Hong and C.H. Hyun, *Phys. Rev.*, **C74** (2006) 025809.

[19] C. Angulo, M. Arnould, M. Rayet et al. (NACRE collaboration), *Nucl. Phys.*, **A656** (1999) 3; http://pntpm.ulb.ac.be/Nacre/nacre.htm.

[20] R. Longland et al.; Iliadis et al., *Nucl. Phys.*, **A841** (2010) 1–388.

[21] P. Descouvemont, A. Adahchour, C. Angulo, A. Coc and E. Vangioni–Flam, *At. Data Nucl. Data Tables*, **88** (2004) 203.

[22] R.H. Cyburt, *Phys. Rev.*, **D70** (2004) 023505.

[23] P.D. Serpico, S. Esposito, F. Iocco, G. Mangano, G. Miele and O. Pisanti, *Journal of Cosmology and Astroparticle Physics*, **12** (2004) 010.

[24] D.S. Leonard, H.J. Karwowski, C.R. Brune, B.M. Fisher, and E.J. Ludwig, *Phys. Rev.*, **C73** (2006) 045801.

[25] R.H. Cyburt and B. Davids, *Phys. Rev.*, **C78** (2008) 064614.

[26] A. Di Leva, L. Gialanella, R. Kunz et al., *Phys. Rev. Lett.*, **102** (2009) 232502.

[27] M.S. Smith, L.H. Kawano & R.A. Malaney, *Astrophys. J. S.*, **85** (1993) 219.

[28] R. Esmailzadeh, G.D. Starkman and S. Dimopoulos, *Astrophys. J.*, **378** (1991) 504.

[29] A. Coc, A., E. Vangioni-Flam, P. Descouvemont, A. Adahchour and C. Angulo, *Astrophys. J.*, **600** (2004) 544.

[30] A. Coc & E. Vangioni, *Journal of Physics Conference Series*, **202** (2010) 012001.

[31] R.H. Cyburt, B.D. Fields and K.A. Olive, *Journal of Cosmology and Astroparticle Physics*, **11** (2008) 012.

[32] F. Spite and M. Spite, Proceedings IAU Symposium No. 268, Light Elements in the Universe 9-13 November, Geneva, Switzerland, Eds. Corinne Charbonnel, Monica Tosi, Francesca Primas & Christina Chiappini Cambridge University Press, p. 201.

[33] R.N. Boyd, C.R. Brune, G.M. Fuller and C.J. Smith, *Phys. Rev.*, **D82** (2010) 105005.

[34] N. Chakraborty, B.D. Fields and K.A. Olive, *Phys. Rev.*, **D83** (2011) 063006.

[35] C. Angulo, E. Casarejos, M. Coude, P. Demaret, P. Leleux, F. Vanderbist, A. Coc, J. Kiener, V. Tatischeff, T. Davinson, A.S. Murphy, N.L. Achouri, N.A. Orr, D. Cortina-Gil, P. Figuera, B.R. Fulton, I. Mukha and E. Vangioni, *Astrophys. J. Lett.*, **630** (2005) L105–L108.

[36] P.D. O'Malley, D.W. Bardayan, A.S. Adekola et al., *Phys. Rev.*, **C84** 042801(R).

[37] O.S. Kirsebom and B. Davids, *Phys. Rev.*, **C84** (2011) 058801.

[38] A. Coc, N.J. Nunes, K.A. Olive, J.-P. Uzan and E. Vangioni, *Phys. Rev.*, **D76** (2007) 023511.

[39] F. Hammache, M. Heil, S. Typel et al. *Phys. Rev.*, **C82** (2010) 065803.

[40] A. Coc, S. Goriely, Y. Xu, M. Saimpert and E. Vangioni, *Astrophys. J.*, **744** (2012) 158.

[41] M. Asplund, D. Lambert, P.E. F. Nissen, F. Primas and V. Smith, *Astrophys. J.*, **644** (2006) 229.

[42] F. Hoyle, *Astrophys. J. S.*, **1** (1954) 121.

[43] C. Iliadis, *Nuclear Physics of Stars* Wiley-VCH Verlag, Wenheim, Germany, 2007, ISBN 978-3-527-40602-9.

[44] H. Oberhummer, A. Csòtò and H. Schlattl, *Nucl. Phys.*, **A688** (2001) 560.

[45] H. Schlattl, A. Heger, H. Oberhummer, T. Rauscher and A. Csòtò, *Astrophysics and Space Science*, **291** (2004) 27.

[46] S. Ekström, A. Coc, P. Descouvemont, G. Meynet, K.A. Olive, J.-Ph. Uzan and E. Vangioni, *Astron. Astrophys.*, **514** (2010) A62.

[47] D. Dicus, E. Kolb, A. Gleeson, E. Sudarshan, V. Teplitz and M. Turner, *Phys. Rev.*, **D26** (1982) 2694.

[48] V. F. Dmitriev, V. V. Flambaum and J. K. Webb, *Phys. Rev.*, **D69** (2004) 063506.

[49] P.J. Peebles and R.H. Dicke, *Phys. Rev.*, **128** (1962) 2006.

[50] K.A. Olive, M. Pospelov, Y.-Z. Qian, G. Manhès, E. Vangioni-Flam, A. Coc and M. Cassé *Phys. Rev.*, **D69** (2004) 027701.

[51] T. Damour and F. Dyson, *Nucl. Phys.*, **B480** (1996) 37.